The software and hardware architecture of the real-time protection of in-vessel components in JET-ILW

THE SOFTWARE AND HARDWARE ARCHITECTURE OF THE REAL-TIME PROTECTION OF IN-VESSEL COMPONENTS IN JET-ILW

V. Huber[1], A. Huber[2], D. Kinna[3], G.F. Matthews[3], G. Sergienko[2], I. Balboa[3], S. Brezinsek[2], P. J. Lomas[3], J. Mailloux[3], P. McCullen[3], Ph. Mertens[2], F. G. Rimini[3], S. Silburn[3], D. Valcarcel[3], K-D. Zastrow[3] and JET contributors[*]

Email: V.Huber@fz-juelich.de

[1]Forschungszentrum Jülich GmbH, Supercomputing Centre, Jülich, Germany

[2]Forschungszentrum Jülich GmbH, Institut für Energie- und Klimaforschung – Plasmaphysik, Jülich, Germany

[3]CCFE, Culham Science Centre, Abingdon, UK

*See the author list of ″X. Litaudon *et al* 2017 Nucl. Fusion 57 102001″

Abstract

For the first time, the JET operation in deuterium-tritium (D-T) plasma, which is scheduled to take place on JET in 2020, will be performed in the ITER mix of plasma-facing component materials. In view of the preparation of the DT campaign (DTE2), several aspects of the plasma operation require significant improvements, such as a real-time protection of the first wall. The risk of damaging the metallic PFCs caused by beryllium melting or cracking of tungsten owing to thermal fatigue required a new reliable D-T compatible active protection system. Therefore, the future development of the JET real time first wall protection is focused on the D-T campaign and the ITER relevant conditions which may cause failure of camera electronics within the Torus hall. In addition to the technological aspect, the intensive preparation of the diverse software tools and real time algorithms for hot spot detection as well as alarm handling strategy required for the wall protection is in progress.
This contribution describes the improved design, implementation, and operation of the near infrared (NIR) imaging diagnostic system of the JET-ILW plasma experiment and its integration into the existing JET protection architecture. To provide the reliable wall protection during the DTE2, two more sensitive logarithmic NIR camera systems equipped with new optical relays to take images and cameras outside of the biological shield have been installed on JET-ILW and calibrated with an in-vessel calibration light source. Additionally, post-pulse data visualization and advanced analysis of all types of imaging data is provided by the new software framework JUVIL (JET Users Video Imaging Library). The formation of hot spots is recognized as a significant threat due to rapid surface temperature rise. Because it could trigger the protection system to stop a pulse, it is important to identify the mechanisms and conditions responsible for the formation of such hot spots. To address this issue the new software tool “Hotspot Editor” has been developed.

1. Introduction

JET-ILW operation in a deuterium-tritium (D-T) plasma is planned for 2020. In the view of preparation this campaign, a real-time protection of the first wall requires significant improvements. JET-ILW combines plasma-facing components (PFC) made of bulk beryllium for main chamber limiter tiles and of bulk tungsten as well as tungsten coated CFC tiles for the divertor tiles [1]. This is the first time that JET-ILW will perform such an experiment with the ITER mix of plasma-facing materials. To avoid damage of the plasma-facing components caused by beryllium melting or cracking of tungsten owing to thermal fatigue, a new reliable D-T compatible active protection system is required. To address this issue, a real time protection system comprising newly installed imaging diagnostics, real time algorithms for hot spot detection and alarm handling strategy has been implemented into the JET protection system. Considering the different material properties of ILW-PFCs, the real time imaging system must fulfil several objectives such as avoiding the melting of the Be-tiles, minimizing the risk of delamination of the tungsten coated tiles and keeping the surface temperature below the threshold at which bulk tungsten re-crystallizes (1200ºC) [22]. This means that the system which monitors the surface temperature of the PFCs must be active in every plasma discharge. Such a sophisticated protection becomes especially important during the preparation and execution of the experiments of the coming D-T campaign, where stationary plasmas with an additional power of 40MW/5s and with tolerable wall heat loads and impurity concentration are required.

This contribution describes the development of the JET real time first wall protection focused on the D-T campaign and the ITER relevant conditions. It reports about the new ITER relevant mirror based optical system and the new near infrared imaging diagnostic system as well as about its integration into the existing JET protection hardware and software architecture. In addition to the technological aspect, the paper presents the preparation of the diverse software tools and real time algorithms for hot spot detection as well as alarm handling strategy required for the wall protection during the coming D-T campaign. The outline of the present article is as follows. Section 2 introduces the near infrared imaging system on JET-ILW including the cameras located inside the Torus Hall as well as the new D-T compatible systems which are built outside the biological shield. The architectures of the video digitization and distribution as well as the real time protection system are given in sections 3 and 4, respectively. In section 5, we will discuss the first wall overheating events. A classification of overheating

events is introduced. In addition, examples of key hot spot formations that could interfere with the safe operation of JET-ILW during D-T plasmas and examples of real-time protection system activation are discussed. This section also includes the discussion about the reliability of the real time protection system. Section 6 introduces the new D-T compatible NIR imaging system on JET-ILW including the cameras and optical components. It covers also the new strategy for the reduction of the lower detection surface temperature limit as well as the backup solution for real time protection based on forward thermal calculations (WALLS). A description of the software framework JUVIL and other software for data analysis of imaging system is given in section 7. This section is strongly concentrated on the description of new developed Hot Spot Editor tool. Based on this software, the analysis of the key hot spots on the JET machine is given. In addition, the in-vessel calibration of the imaging diagnostics is described in this section. Finally, a summary is given in section 8.

2. Near Infrared Imaging Diagnostic Systems

The JET-ILW imaging system for machine protection is based on two types of cameras:

- 12 protection cameras of the first type are analogue monochrome NIR CCD cameras located inside the biological shield in the JET torus hall:
  - Hitachi KP-M1AP cameras provide non-disturbed operation of CCD sensors and electronics in the presence of a magnetic field.
  - Sensor: Sony ICX423AL, pixel size 11.6μm (H)×11.2μm (V)
  - Synchronized with the external sync signals (V/H scans)
  - The cameras operate in non-interlaced mode at 50 fields per second with binning (odd and even lines are exposed together at the same time). In this mode, the cameras deliver images with an apparent size of 720 × 288 pixels every 20ms.
  - Each of the cameras is equipped with a near infrared (NIR) filter. Two types of band pass filters have been used: 980±10 nm and 1016±40 nm.
  - The cameras can operate without replacement at least one year, withstanding the neutron fluence of ~2×10^{12} n/cm^2 [3].
- The new JET imaging system for machine protection is DT compatible and consist of 2 new digital logarithmic NIR cameras located outside the biological shield:
  - Imaging Technologies (NIT), Widy SWIR 640U-ST cameras
  - Resolution 640×512 pixels, pixel size 15μm ×15μm, max. frame rate 200 fps

- Dynamic range 14bits, USB2 or USB3 data connection interface
- Logarithmic response [4].
- These NIR-SWIR cameras use InGaAs (Indium Gallium Arsenide) detectors, offering a high quantum efficiency (QE>70%) at the wavelength range 900-1700nm. Two types of band pass filters have been used: 1200nm±10nm and 1250nm±25nm.

The entire imaging system comprises four wide-angle views, four tangential divertor views, and three views of the divertor from the top. The cameras are used to measure the surface temperature of the PFCs and act as sensors for the real-time control. The operation temperature ranges of NIR protection cameras for the materials used on JET are: Be 700-1400°C; W coating 700-1370°C; solid W 700-1400°C.

3. Video Digitization and Distribution

A data flow diagram which includes fundamental camera hardware and data processing components is shown in Fig.1. The analogue composite video signal from each CCD camera is digitized by a Gigabit Ethernet (GigE) frame grabber iPORT PT1000-ANL (2-6-V2-E). The frame grabber shares the digital video data across a dedicated network to three separate PCs simultaneously: the camera Real Time Processing system, a Video Capture system for data storage, and the Live Display. This setup is replicated for each Hitachi camera. The risk of failure of these cameras and their electronics within the Torus hall during the D-T plasma operation is very high due to the significant increase of the hard radiation level (neutrons/gammas).

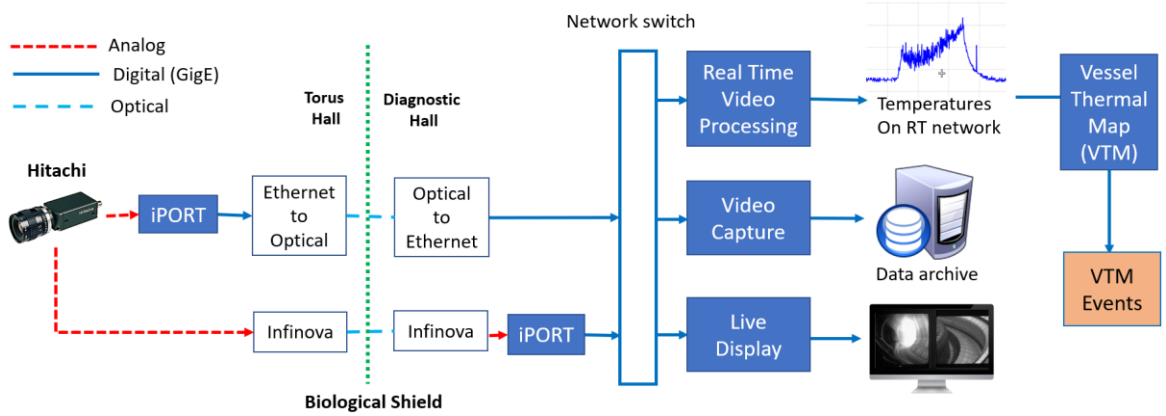

Fig.1. Video digitization and distribution from Hitachi cameras

Note that two identical video cameras are used during the first D-T campaign (DTE1) to view the divertor from windows at the top of the machine: narrow bandpass filters allow one to record D_α radiation, the other CII radiation. One of these cameras failed for technical reasons, but the other survived the DTE1 campaign without significant damage, the neutron fluence in the area being$\approx 6\times10^{12}$ neutrons cm^{-2} (equivalent silicon displacement at 1 MeV fluence). The detailed report about the diagnostic experience during the first deuterium–tritium experiments

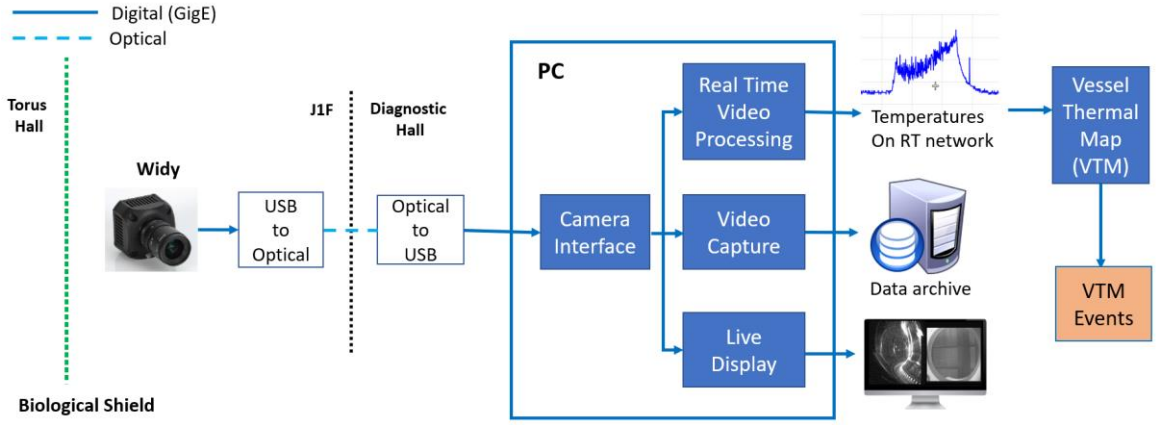

Fig2. Video digitalization and distribution from WiDY cameras

in JET, can be found in [5]. To avoid the risk of a camera failure and provide the reliable wall protection needed during the coming D-T campaign, two camera systems with wide angle and divertor field of view, equipped with new optical relays to take the images and the cameras outside of the biological shield, have been installed on JET-ILW. These new 'Widy' cameras (see Section 2) with logarithmic response are currently under commissioning. They generate digital data directly via USB (see Fig.2). For these cameras, a single PC manages the real time processing, captures and propagates data for live display, using separate processes in a logical structure that mimics the architecture above.

4. The Real Time Protection System Architecture

Fig. 3 represents the architecture of the Real time protection system. A real time processing system on each camera converts pixel intensities to the surface temperature. To provide a faster response, the real-time protection system monitors only Regions Of Interest (ROIs) on the selected PFCs of different materials. The maximum temperature measured in each ROI is sent to a separate real time system known as the Vessel Thermal Map (VTM) [6]. If the temperature from an active ROI of some camera crosses a threshold for a vessel wall segment, the VTM classifies this as a 'Main chamber Hot Spot' or a 'Divertor Hot Spot' depending on where the event happens and triggers an alarm. It is the VTM that communicates with the Real-Time

Protection Sequencer (RTPS), which in turn decides how the control actuators should respond. The response of the RTPS is programmable and takes into account many inputs in addition to those from imaging diagnostics. The action is usually not a hard, fast stop, but instead a pre-programmed controlled plasma termination, called ‘soft landing,’ to mitigate a disruption. The

Fig.3. The architecture of the Real time protection system.

algorithm for real-time image processing and elimination of pixels which should not contribute to the calculation because they are caused by sensor aberrations or transient phenomena such as neutron hits, and its implementation, are described in [7]. The entire system including the selection of wall segments and corresponding ROIs, alarm thresholds as well as RTPS responses is highly configurable. A special tool, so called "Level 1", enables to set-up the configuration and to verify the consistency of the configuration settings.

5. First Wall Overheating Events

5.1 Classification of the overheating events

The aim of the real-time protection system is to provide a reliable protection of the bulk material components and of the tungsten-coated tiles of the first wall against overheating. In particular, the formation of so-called hot spots, the localized regions on the first wall components with higher temperatures than the surrounding regions, should be avoided regardless of the magnetic field configurations or plasma scenarios.

Two types of the hot spots are considered:

 The first type of overheating could lead to a severe damage of the wall tiles and requires protection. In this contribution we will call such overheating events as genuine hot spots, which include:

- Overheating events caused by heat flux overload of wall components
- Genuine hot spots induced by fast particle loss from the NBI and ICRH heating.
- Genuine hots spots resulting from overheating of the wall component edges. There are leading edges at wall components due to small misalignment of components exceeding the engineering tolerances during their assembly.

 The second type of overheating associated with a surface temperature increase due to other causes than genuine overheating. We will call such overheating events false hot spots caused by the following conditions:

- Dust particles on the surface become quickly very hot due to poor thermal connection with the underlying material. The hot dust particles do not have any impact on the machine operation generating false hot spots.
- Overheating of the re-deposited layers does not pose any risk to the integrity of the plasma-facing components but may result in false alarms. Re-deposited layers onto plasma-facing wall elements have low thermal capacity and a poor thermal contact with the underlying material. Therefore, even the low heat flux exposure could lead to high-temperature hot spot formation.
- Overheating of the flakes, droplets and jagged edges, which could result from delamination of the coating, will not severely damage the first wall. Therefore, the hot spots generated by delamination of the coating are considered as false hot spots.

5.2 Main hot spots considered as a large threat during DT-campaign

In this section examples of key hot spot formations that could interfere with the safe operation of JET-ILW during D-T plasmas are discussed and examples of real-time protection system activation are given. Figure 4 shows wide angle NIR images of the JET in-vessel PFCs using the JET NIR systems. These images show different cases of hot spot formation on the first wall components.

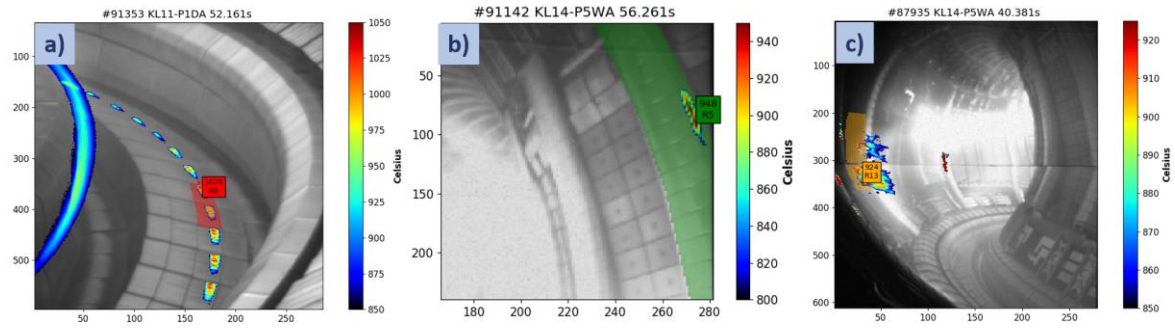

Fig.4 a) Classical heat up of the divertor W bulk tiles, b) Hot spot on the inner wall guard limiter (IWGL), c) Hot spots on the NBI beam re-ionization zone.

The image on Fig.4a illustrates a typical classical heat-up of the divertor bulk tungsten tiles. We describe in this contribution the heat-up process as classical when the response of the surface temperature demonstrates a slow increase and reduction by applying and removal of

the heat load source correspondingly. The hottest areas correspond to the location of the outer strike point on the bulk tungsten tiles, where the heat flux is maximal. The recorded video was obtained from an H-mode discharge (JET pulse #91353) with an auxiliary heating of 12 MW in magnetic equilibria: $B_T \approx 2.7$T, I_p=3.2 MA, q95= 3.58. Fig.5 shows the time evolution of this H-mode discharge in JET-ILW demonstrating the surface temperature increase with time during the auxiliary heating phase. For avoiding false alarms due to spurious signals on the camera image (e.g. caused by neutron impact), VTM checks that the monitored temperature is consistently above the trip level during a certain time window, which is called "assertion time." In this case the trip level was defined as 975ºC to keep the surface temperature below threshold at which the bulk tungsten re-crystallizes (1200ºC) and the assertion time was set to 400ms. After the trip level was reached at time 12.2s the surface temperature remains above the trip level for longer than the assertion time. The VTM sends an alarm to RTPS and requests an appropriate action from the plasma control systems. RTPS decided for the plasma termination, the so-called soft landing: the auxiliary power was switched off, the strike points moved away, and the plasma current was ramped down. The maximal value of surface temperature reaches the value of 1030ºC, which is significantly below the value at which the bulk tungsten re-crystallizes (1200ºC).

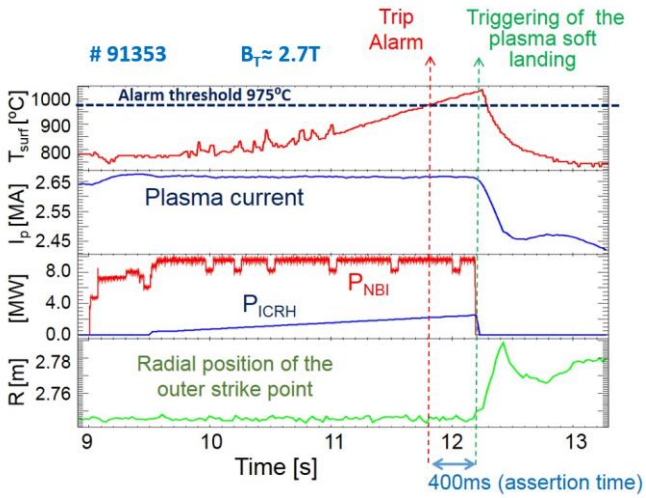

Fig.5 A discharge with a classical heat up of the divertor tungsten bulk tiles.

Figures 4b shows the images taken during an ohmic discharge with a hot spot formation on the inner beryllium limiter. At the time of 16.1s, the surface temperature of the Be limiter reaches the trip level of 925°C and remains longer than the assertion time of 200ms above this trip level (see Fig. 6). At time 16.3s, VTM sends an alert to RTPS requesting the recovery action from

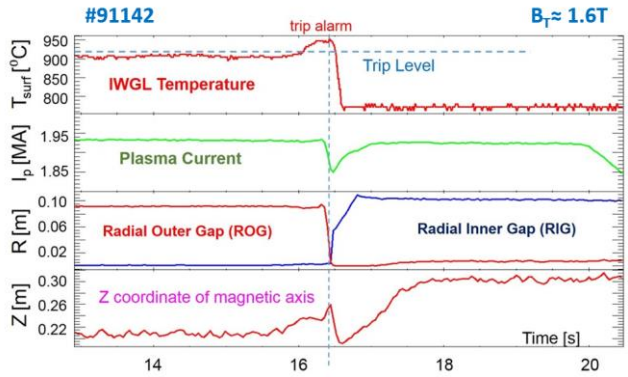

Fig.6 ROI temperature, the plasma current, radial outer and inner gaps of the plasma position during a hotspot formation on the inner beryllium limiter (IWGL)

the plasma control systems. Consequently, the plasma is shifted outwards. The cooling of the Be tiles after moving the plasma and correspondingly switching off the heat loads takes place very quickly. This very fast thermal response to the applied or removed power loads is due to the low thermal capacity of the thin layer and its lack of thermal attachment to the bulk material. The plasma current I_p signal shows a slight drop due to the change of the plasma internal inductance (l_i) during the plasma movement. After 0.5s the plasma controller forces I_p to the requested value. The plasma discharge was not terminated and thus, the RTPS recovery action was successful.

Figures 4c shows the hot spot formation on the NBI beam re- ionization zones. A fraction of the injected neutrals has been ionized in the plasma edge outside the separatrix before its entrance into the plasma. They drift and then impinge on specific tiles near the outer wall poloidal limiters. These tiles are referred to as beam re-ionisation zones and are made of W-coated CFC. Estimations for 8 D beams at 130 kV and used at high density (around 10^{20} m^{-3}) [8] shows that the peak power density on these areas could be in the range of 5.5 to 23 MW/m^2 depending on the limiter - plasma separatrix distance (8 to 5 cm). From the analysis of the response of the surface temperature on the heat loads, we can conclude that the re-ionisation zone demonstrates a classical heat up and cool down behaviour: a slow increase of the temperature by applying heat loads as well as a slow temperature reduction after removal of the heat load source. To avoid the overheating due to re-ionisation, the plasma is softly terminated by switching off the auxiliary power and ramping down the plasma current.

5.3 Reliability of the real-time protection system

All VTM alarms on the JET-ILW machine are well characterised and catalogued since the C31 campaign (2013) when the Real-Time Protection system started to operate routinely.

Fig. 7 shows the number of alarms per bin of 500 plasma discharges. The genuine alarms include the genuine hot spots as well as classical heat load events which demonstrate a classical heat up and cool down behaviour: a slow increase of the temperature by applying heat loads as

well as a slow temperature reduction after removal of the heat load source. A large number of VTM alarms were triggered during the first 3 campaigns, C31, C32 and C33. The majority of these alarms was due to classical heat up of the first wall components, due to hot spot formation and due to heating of the NBI beam re-ionization zones (see Fig.7b and 7c). The classical heat up of the wall components occurred mainly during the H-mode plasmas with additional neutral beam as well as ICRH heating. In the early pulses, the predominant location of the alarms in the divertor region was the divertor tile 5 (horizontal target) while later, the number of alarms from tile 6 signals increased significantly. Around the 86501 and 87000 pulse marks, an increased number of alarms was noted, mostly triggered by temperature signals from divertor tiles 5, 6 and 7. The maximal number of alarms of about 70 was triggered at mark 87001 which correspond to the pulse range of 87001-87500. During this pulse range about 14% of plasma discharges were terminated to avoid harmful situations like dangerous overheating through classical heat up of the wall components. Averaged over the entire C33 campaign, about 8% of the plasma discharges were terminated by RTPS. Also, the number of alarms due the NBI beam re-ionization during the C33 campaign reached the maximum of 2-3%.

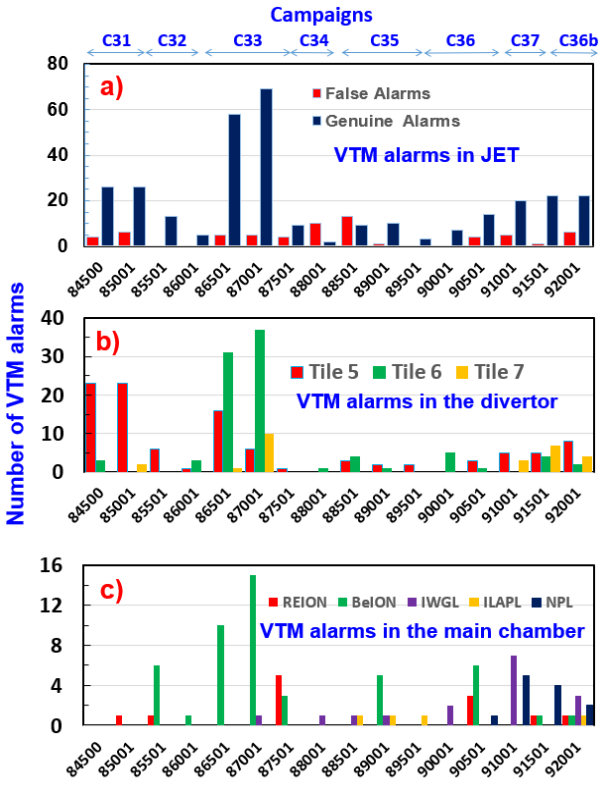

Fig.7 Number of a) total VTM alarms b) in the main chamber and c) in the divertor region

The statistic of the VTM alarms show a general tendency of reduction during the following campaigns C34-C36. There are two main reasons for these significant improvements. First, the real-time protection system undergoes a continuous improvement. Second, a better understanding of the physics of the overheating events that cause the alarms provides the guidelines for the safe operation of the JET machine. In the last experimental campaigns C37 and C36b, a significant improvement of the auxiliary heating systems on JET-ILW was carried out, resulting in a marginal increase in plasma terminations due to the RTPS safety system. During this period, there are about 2-3% plasma terminations due to the classic heat up events and about 1-1.5% stops due to the formation of hot spots. Although overall additional heating has

increased significantly in these campaigns, false alarms have been reduced to less than 0.5% of all plasma discharges.

6. Real-Protection of the First Wall for DT-Campaign

6.1 Near-Infrared SWIR Logarithmic Imaging Diagnostics Systems

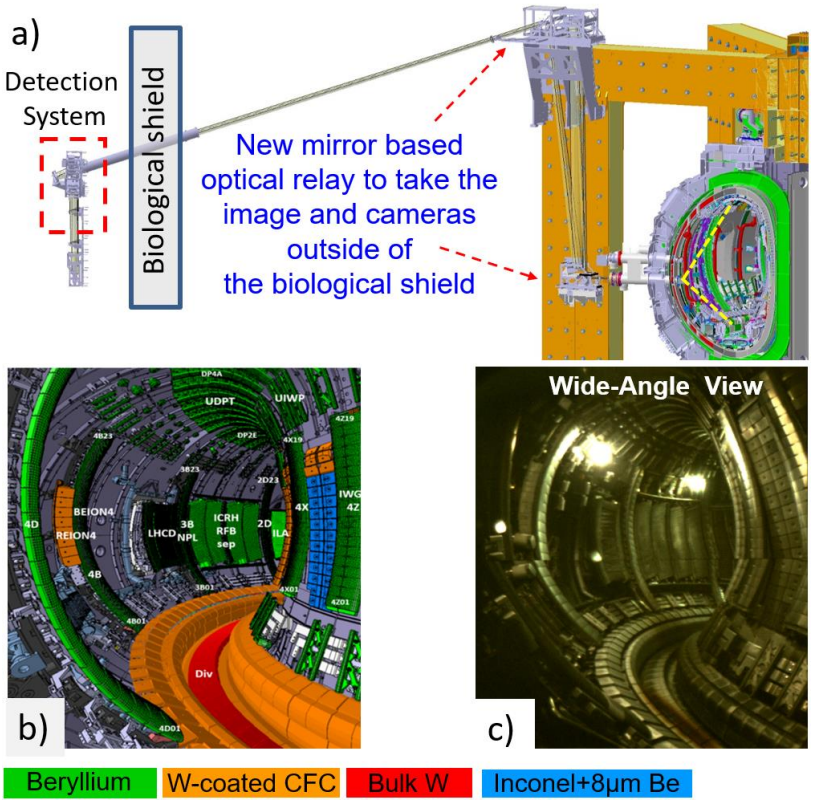

Fig.8. a) Mechanical layout, b) field of view, c) camera image of the wide-angle imaging system.

The future development of the JET real-time first wall protection is focused on the D-T campaign and on operation near ITER relevant conditions. D-T operation at JET will cause failure of camera electronics within the Torus hall due to significant increase of the hard radiation level (neutrons and gammas). To provide the reliable wall protection needed during the coming D-T campaign, two camera systems, equipped with new optical relays to take the images and the cameras outside of the biological shield, have been installed on JET-ILW and calibrated with an in-vessel calibration light source [9, 10]. The optical design concept of both systems with wide angle view as well as the divertor view is based on reflective optics, mainly to be able to sustain high neutron radiation. The reflective optics were also chosen to avoid chromatic aberrations. Similar to the ITER conditions, it transports the light by reflective optics (mirror systems) over long distances (>40 m) to the detection system located outside the biological shield. Figures 8 and 9 show the mechanical layout and fields of view of the wide-angle and of the divertor imaging systems, respectively. These figures represent also fields of view of the new imaging systems. Different colours represent the different materials of the first wall: green – beryllium; red –bulk tungsten; orange –W-coated CFC; blue – Inconel coated with 8µm Be. The wide-angle system contains an in-vessel mirror box with three stainless steel mirrors coated with rhodium (Rh) which view

the torus through a conically shaped aperture. Rh mirrors have a high reflectivity (70-80%) in the visible spectral range [11] as well as in the near-infrared and infrared ranges (around 85% at 1μm). Rhodium has also a low chemical reactivity, preventing oxide and carbide formation [12, 13]. Due to the aforementioned optical and chemical properties, rhodium is considered to be an important candidate material for first mirrors in ITER [14, 15,16]. The mirrors of the ex-vessel optics of both imaging systems are made of aluminium to cover the spectral range up to 2500nm. The location of the cameras outside the biological shield makes it possible to integrate more sensitive and sophisticated cameras in the wall protection system. The new JET imaging system for machine protection is equipped now with new digital logarithmic NIR cameras: New Imaging Technologies (NIT), Widy SWIR 640U-ST and 640V-ST cameras, resolution 640×512, pixel size 15μm ×15μm, max. 200 fps, dynamic range 14bits, USB2 or USB3 data connection interface, logarithmic response [4]. These NIR-SWIR cameras use InGaAs (Indium Gallium Arsenide) detectors, offering a high quantum efficiency (QE>70%) at the wavelength range 900-1700nm. For these cameras, a band pass filter 1200nm±10nm is used. The choice of the camera and the central wavelength of the filter is based on the analysis reported in [7]. There are advantages of the usage of the optimised wavelength (λ=1.2μm) for the surface temperature measurements: especially the temperature independent spectral emissivity of tungsten. The so-called "X-point of W", where the emissivity wavelength isotherms cross, corresponds to λ≈1.27 μm and it is very close to the chosen wavelength of 1.2 μm. Additionally, the operation in the NIR wavelength range made the surface temperature measurements less sensitive to the surface roughness.

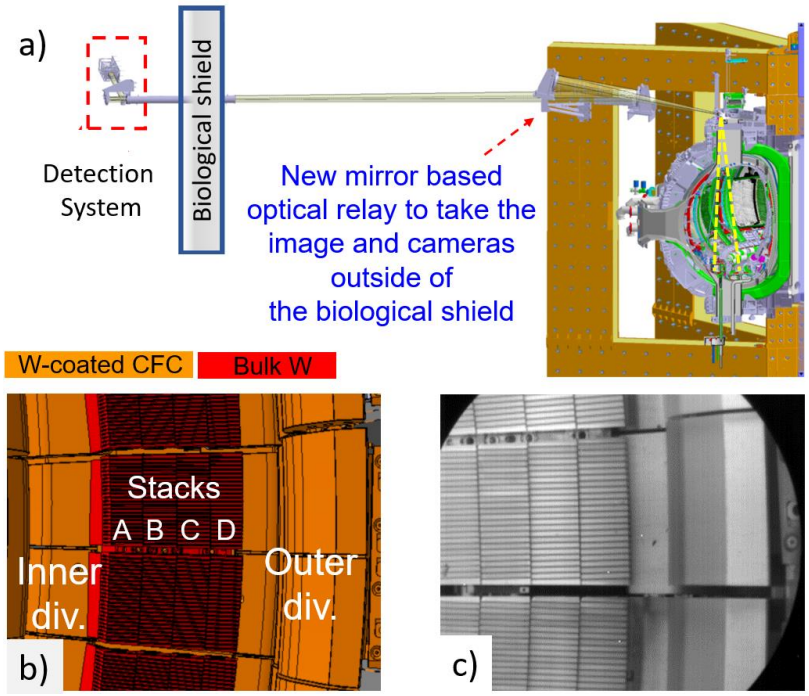

Fig.9. a) Mechanical layout, b) field of view, c) camera image of the divertor imaging system.

Also in contrast to MWIR detection, the usage of the NIR wavelength reduces the maximum relative error. The detailed analysis for the selection of the optimal wavelength range for the protection imaging is given in [7]. All camera sensors are cooled to temperatures of about 0°C to reduce the dark noise which is less at lower temperatures. One example of the calibration of the wide angle Widy camera by an in-vessel calibration light source (ICLS) is shown in Fig.10a: digital levels measured by the camera versus brightness temperatures of the ICLS with one lamp and with a combination of two lamps. The Planck radiation curve was used as a fit of the experimental data. The calibration curve could be easily adapted to the wanted material as shown in Fig.10a: yellow for W coated, red for bulk tungsten and green for beryllium. During the calibration, it was recognised that the selected InGaAs sensor is sensitive to changes of sensor temperatures as shown in Fig.10b. For the sensor temperature of 0°C the camera demonstrates a higher sensitivity. Consequently, cameras were calibrated for several sensor temperatures and times exposures which will be used during the experiments.

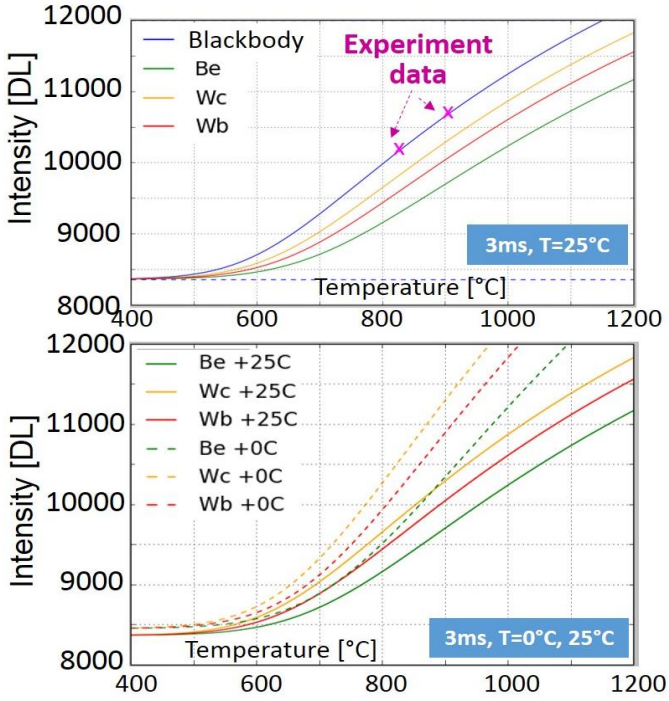

Fig.10. a) Digital levels measured by the camera versus brightness temperatures of the ICLS with one and two lamps b) Calibration for sensor temperatures: 0°C and 25°C.

6.2. Improvements to the Protection System: Dynamic Background

In order to convert pixels intensities to a surface temperature, the RTPU applies the following configuration settings for each camera: ROI pixel map, dead pixel map, flat field map, background mean dark values, and calibration look-up tables for the materials installed on JET. The pixel intensity used for look-up is first corrected for the 'dark field' offset (background) and for variations in pixel response to illumination by applying the following formula:

$I_{real} = (I-\alpha)/\beta$, where I is the measured intensity, α is the background offset and β is the flat field correction. Historically, the configuration files for JET cameras are installed and stored in 'Level 1' as 'static' files to provide the reliability of the protection system against possible failures. But the post-pulse analysis of the dark field background shows that it significantly

changes with time due to the evolution of hot pixels from impact of neutrons [3]. That was confirmed by comparison of the camera images in JUVIL (see section 7.1) by applying the static background from Level 1 and dynamical background calculated as an averaged frame of the first 100 video frames. The Figures 11a and 11b show that the dynamical background enables to improve the image contrast and visibility of hot spots. Furthermore, it provides the possibility to reduce the detection limit of measured temperatures thanks to the reduction of the background 'noise' (see Fig 11c and 11d).

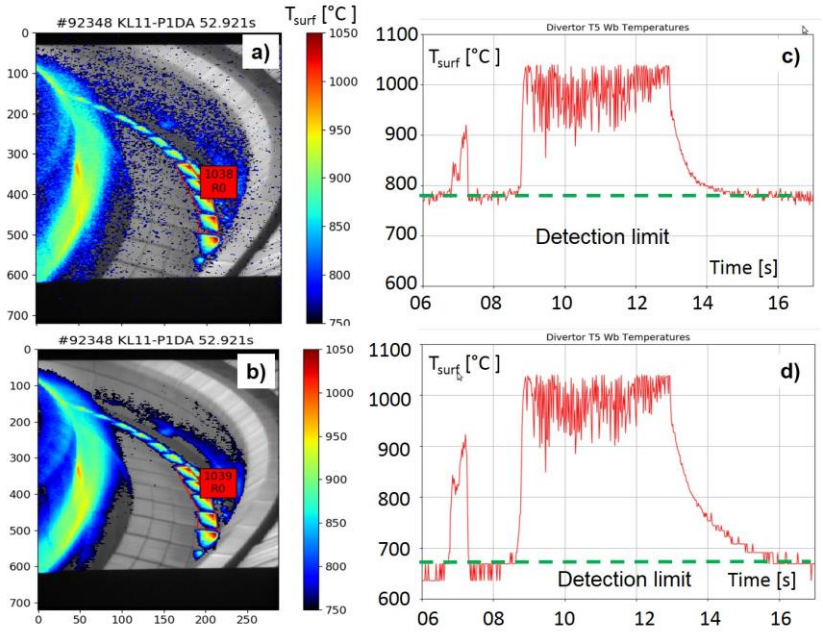

Fig.11. Surface temperature distribution, profile and detection limit after applying a,c) the static and b,d) the dynamic background.

Therefore, it is useful to generate the dynamic background for the real-time system during each pre-pulse stage in order to increase the temperature range measured by the NIR cameras.

6.3. Real-time protection based on forward thermal calculations (WALLS)

In addition to the real time protection system based on the NIR imaging, further backup will be provided by an improved real-time protection based on forward thermal calculations (WALLS) [17]. The backup solution becomes especially important if some video systems fail during the D-T operation. WALLS is a real-time system that takes measurements of magnetic sensors (for equilibrium calculations), input power, thermocouples and total radiated power to compute heat loads onto plasma-facing components and the magnetic field geometry on the divertor. Limits are then checked with an alarm being raised if they are exceeded.

At the moment WALLS protects the tiles in the Inner Wall Guard Limiter (IWGL) and wide outer poloidal limiter (WOPL) against high surface temperature. Divertor tiles are protected against reaching high energy limits and against having the field line angle too steep, thus avoid exposing the gap between tiles to power loads.

Currently, WALLS is used routinely in JET operation and is being updated to include surface temperature protection of the outer horizontal divertor tile.

7. Post-pulse Data Visualization and Advanced Analysis

7.1 JUVIL Video Imaging Software

The JUVIL (JET Users Video Imaging Library) framework [18] provides graphical components and functions for loading and post-processing of video data from various imaging systems installed on JET. Due to the separation between generic interfaces and site-specific implementations, the system is highly configurable and can be extended and adapted for new imaging cameras and data formats. It provides easy access and post-processing functions for video data, which is quite important for the development of new applications for users' own analysis. Fig. 12 shows the JUVIL video player which displays the data from protection (NIR), operation (CCD colour) and scientific (IR and VIS) cameras; intershot videos, data recorded during camera calibration experiments, as well as tomographic reconstructions from the bolometer and VIS cameras. To improve the performance the videos are loaded in chunks of 100 frames. The initial time is synchronized to the time of the previously loaded video to enable quick comparison of the images from several cameras. The JUVIL automatically carries out the video post-processing (e.g. if necessary, the frames are rotated), and shows to a user the information about camera and video settings. It also converts the digital level counts of video pixels to the real temperatures by applying of the same algorithm as the real time processing system does: subtracts the dark current background, performs dead pixels and flat field corrections, and maps the results to the temperatures of materials in look-up tables. If the pre-pulse video background is not available, JUVIL calculates it as an average frame of first video frames assuming the temperatures at the beginning of the pulse are low and not visible by JET cameras. Furthermore, the user can select the upper temperature range to be displayed. It enables to show a camera image usually taken during disruption underneath the video data to see the distribution of hot regions inside of the vessel. In addition, it is also possible to overplay the video with a vessel structure image generated by the mapping software [19] and see the names of corresponding VTM tiles by moving the mouse inside of the image.

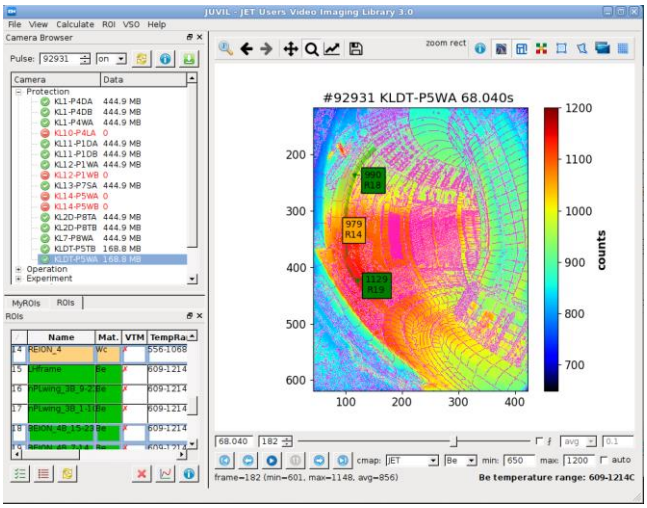

FIG.12. JUVIL 91160 graphical Interface

The JUVIL also loads pre-defined ROIs monitored on each protection camera by a real time processing system, as well as pre-defined analysis ROIs for scientific IR cameras, and shows their locations and temperatures. Thereby, it takes in account the detected camera shake of IR imaging systems using signals stored in JET data base and displays ROI locations and temperatures adjusted to such movements. In addition, a user could dynamically create and store their own ROIs, modify their shapes, locations and other attributes. The maximum or average temperature for IR cameras or digital level for any camera within these ROIs can then be calculated and stored to the JET data base. Furthermore, JUVIL can load from the JET data store and display the peak power loads on divertor tiles calculated from the scientific IR cameras. In addition, there are various functions for users' own analysis of video data, e.g. calculation of maximum, average, and standard deviation profiles of ROIs and video frames.

7.2 VSO Tools

The primary role of the viewing system operator (VSO) is to assist the session leader, engineer in charge and scientific coordinator in the interpretation of an alarm sent by the VTM due to

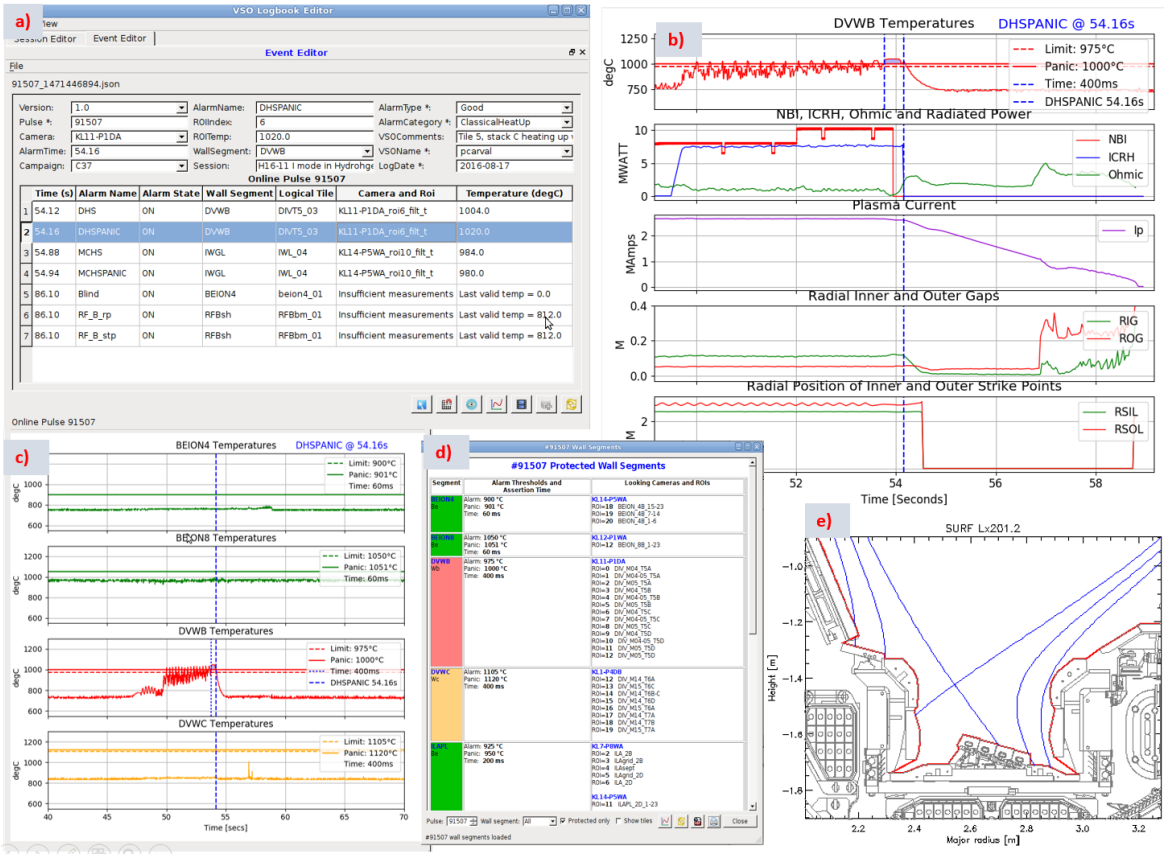

FIG.13. a) The list of VTM alarms raised during the pulse 91507; b) The temperature profile and thresholds of divertor wall segment which raised an alarm including plasma configuration signals (power, plasma current, etc); c) Temperature profiles, thresholds and assertion times of all wall segments; d) The configuration of wall segments with the list of looking cameras and ROIs; e) The corresponding camera video of divertor and the ROI responsible for the VTM alarm loaded automatically.

the protection system during experiments. To simplify the job of the operator, some new features, the so-called VSO tools [16], were integrated into JUVIL for the interpretation of VTM events and for the quick post-pulse analysis of video data from the protection cameras required for the preparation of the next plasma pulse. They enable to load automatically the list of VTM alarms raised for a specific pulse, plot the plasma configuration and temperatures of wall segments with the corresponding alarm thresholds and assertion times, load automatically the video from a protection camera and display a location and temperatures of a ROI caused the VTM alarm (see Fig 13). This saves a significant amount of time, which can be used by the VSO for actual analysis of the event. After the analysis, a VSO stores a categorised VTM alarm to the VSO logbook which provides search and filter functions for all VTM alarms recorded on JET and can display their characteristics and corresponding videos.

7.3. Tools for the Study of Hot Spots

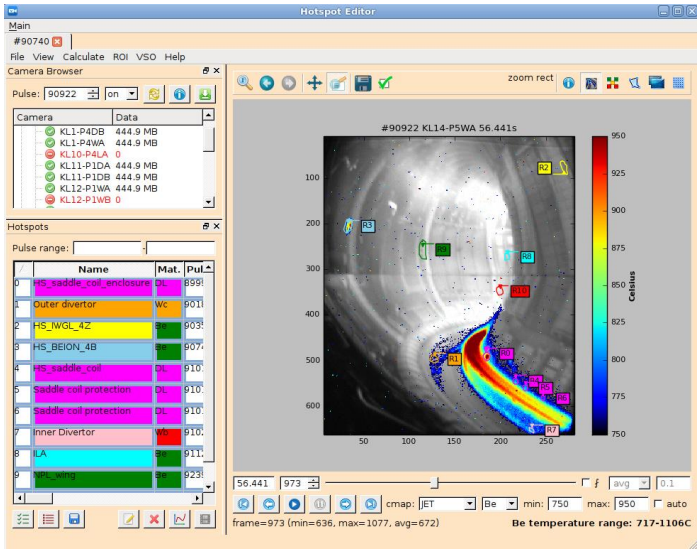

Fig.14. Hotspot Editor

The hot spots are localized regions on the first wall components with higher temperatures than the surrounding regions. Often the hot spots trigger VTM alarms, which may result in a termination of the plasma pulse which may not be necessary. In order to avoid unnecessary stopping of the plasma discharge, it is important to investigate the cause of new hot spots, their locations and temperatures, and the conditions under which the existing hot spots disappear. For this aim, the new Hotspot Editor and Viewer, were integrated into JUVIL [18]. The Hotspot Editor automatically loads the hot spots for a specific camera stored in the catalogue (see Fig.14). The attributes of hot spots are similar to ROIs, but they contain in addition the time when a hot spot was detected or modified, the measured temperature, the flag whether a hot spot caused a VTM alarm, and optionally the time when a hot spot clearly disappeared (e.g. after the cleaning up or the replacement of tiles). It is possible to load automatically the corresponding videos from times when a hot spot was detected or modified. The Hotspot Editor is designed for the analysis of hot spots with temperatures below as well beyond the trip level. It calculates temperatures of hot spots for an arbitrary pulse as

well as enables to plot or store the history of temperatures for specific pulses or pulse range using a thresholding technique to study the temperature evolution of hot spots.

The Hotspot Viewer displays the catalogue of all detected hot spots and shows their development. It provides also the filter options for extraction of hot spots during a pulse range.

7.4. Hot Spot on the Inner Wall Guard Limiter

Fig. 15a shows an example of a hot spot in the main chamber of JET. The clear evidence of the hot spot event is observed at the upper part of the inner wall guard limiter (IWGL). Thanks to the Hotspot Viewer, the evolution of this specific hot spot could be followed (see Fig.15b). The first time this IWGL hot spot was observed was during an ohmic discharge at pulse number 87643. In this pulse the surface temperature of the Be tile reaches the trip level of 925ºC and remains above this trip level for a time window shorter than the assertion time of 200ms. Correspondingly, the alarm was not triggered during this pulse. During the following pulses (e.g. #87728), the surface temperature remained beyond the trip level longer than the assertion time (see Fig.15c). As a consequence, the trip alarm is triggered and VTM sends an alert to RTPS requesting a recovery action from the plasma control systems. The action of the real-time protection system during this hot spot formation is described in detail in section 5.2. The action of the real-time protection system during this hot spot formation is described in detail in [6]. The T_{surf} shows a rapid initial increase, indicating that the measurement is not the result of the thermal heat radiation from the bulk. Such a temporal response of temperature (rapid increase and decrease) is the typical indication for a deposited layer having poor thermal contact with the material substrate. The analysis shows

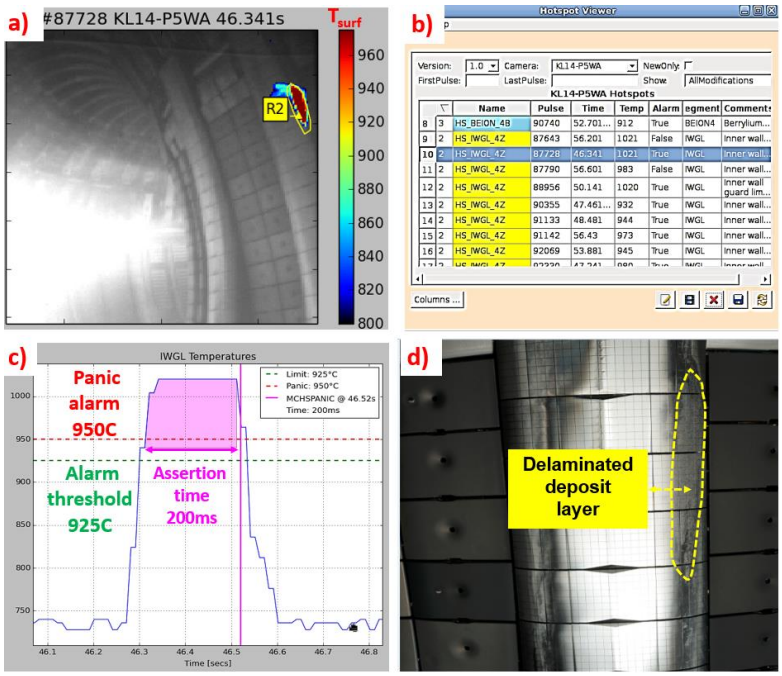

Fig.15. a) Hot spot on the inner wall guard limiter (IWGL); b) Hotspot Viewer catalogue of detected hot spots; c) Surface temperature of the IWGL hot spot; d) High-resolution image of the inner wall guard limiter.

also the slight growth of the size of IWGL spot. It could be explained by the progressing delamination of the deposited layer from the bulk material substrate. That was confirmed by the high-resolution images taken during the vessel survey (see Fig.15d).

7.5. Hot spot on the ITER-like Antenna

Figure 16 shows the hot spot behaviour on the ITER like antenna (ILA) in a pulse range spanning over 5000 pulses. The ILA is one of the additional heating systems at JET which was designed to couple 7.2MW (8MW/m^2) across the frequency range 30-55MHz [20]. Hot spots are the potentially most dangerous events related to ILA operation. If left uncontrolled they can produce damage and cause plasma disruption by exaggerated impurity influx.

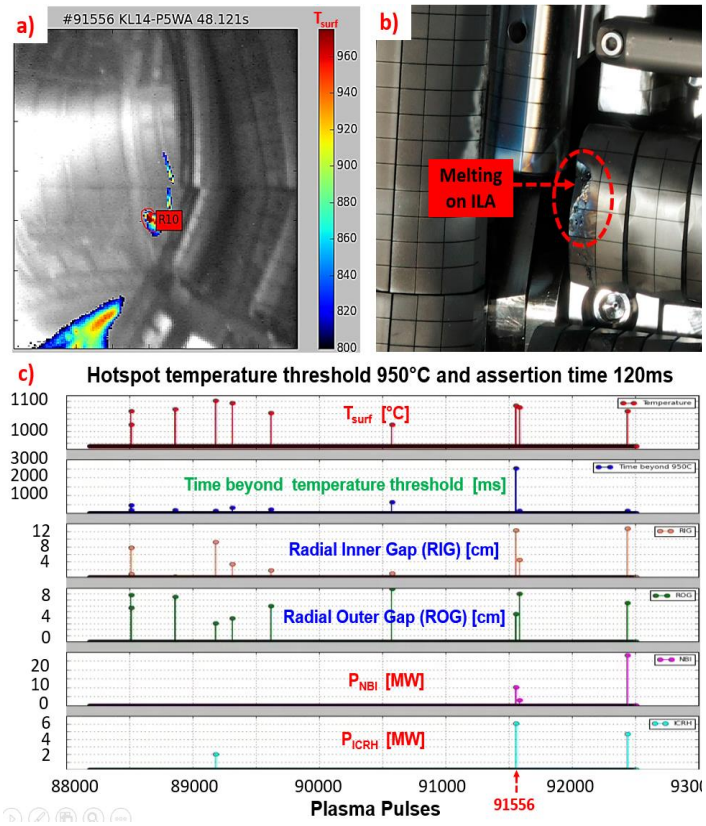

Fig.16. Analysis of the hot spot on the ITER like antenna in a pulse range from 88000 to 92504.

The surface temperature threshold was set for this analysis to 950°C and the assertion time to 120ms. To exclude the hot spots during disruptions, these criteria were cross-checked with the disruption database which contains the full information about disruptions: pulse, time, etc.

Fig. 5c demonstrates the formation of 10 hot spots on the antenna grids and how they correlate with plasma shape parameters: Radial Inner and Outer Gaps (RIGs and ROGs) which define the distance between the inner and outer limiter, respectively, and the plasma. Furthermore, it shows the values of the additional heating power by NBIs and ICRH heating systems. The hot spots around the pulse 89000 were formed in the pulses with small RIG and large ROG values. Additionally, the temperatures remained beyond the temperature threshold for relatively short times: below 300ms. These are indicators that these hot spots have causes which are not related to the overheating of the antenna components. Analysis shows that these hot spots were triggered by

the bremsstrahlung during the wall MARFE formation at the end of the plasma discharge during the disruption phases. They are clearly “false hot spots”. This knowledge was used to deselect such hot spots from the data base. The genuine hot spot at pulse 91556 is related to the overheating of the antenna corner tile of Faraday screen.

7.6. Hot Spots on the Partly Delaminated Divertor Tiles

Fig. 17b shows an image, taken during the in-vessel inspection with high resolution camera, with delamination along CFC fibre planes in a toroidal orientation along the tile. Such altering of the tungsten coating was observed after the campaigns in 2013-2014 [21]. The reason for such a degradation of the divertor coating could be the notable heat loads on this location. It cannot be explained by the carbidisation mechanism, where the surface temperatures should exceed T_{carb}=1350°C for more than two hours [20]. To avoid damage of the coating, the typical alarm temperature thresholds used for the real-time protection on W-coated CFC is 1105ºC which is below this temperature T_{carb}. Delamination along fibre planes is also created by a fatigue due to the mismatch in thermal expansion and is intrinsically variable due to complex 3D structure of CFC materials. Fig.17a shows the mapping of hot spots detected on the divertor. Most of these hot spots form during the ELMy H-mode plasma discharge ($B_T \approx 2.6$ T, I_p=2.5 MA) with the additional input power of about 18.0 MW in low-triangularity magnetic equilibria with the strike points located on the vertical targets. The surface temperature of the hot spots demonstrates a typical behaviour of overheated edges of delaminated layers: quick rise during the ELM and abrupt cool down when the ELM is over. The ELM frequency f_{ELM} in the shown case is ≈15Hz. The hot spots induced by 15Hz ELMs are seen on every third image frame. The protection system does not trigger a VTM

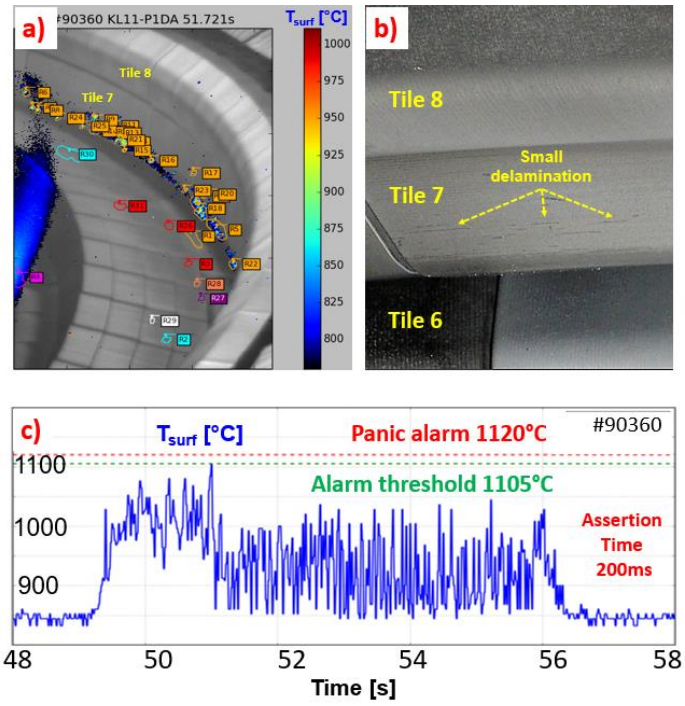

Fig.17. a) Hot spots on the lower outer vertical target (Tile7) during the ELMy H-mode plasma discharge; b) Delamination of W coatings; c) Measured surface temperature profile of Tile 7.

alarm because the temperature of the hotspots remains below the trip level of 1105 ° C during the entire pulse (Fig.17c). Even if the temperature of the hot spots would have exceeded the temperature threshold, the system would not have triggered an alarm. This is because at such ELM frequencies the time duration when the surface temperature is above the trip level is shorter than the assertion time. Since the NIR cameras used for protection [7] work in non-interlaced mode at 50 fields per second, ELMs with a frequency below 25 Hz result in a transient hot spot formation during alternate frame images and therefore ignored by the protection system. We can conclude that for plasmas on JET-ILW with an available additional heating power of ≈28MW and the heating power duration according the JET-ILW requirements, the edge-localized modes with a frequency ≥25 Hz do not increase the T_{surf} to values above the trip level. Therefore, the operation on JET-ILW is generally not limited by the delamination of the tungsten coating on the divertor tiles.

8. Summary

As part of the preparation of the JET-ILW operation in Deuterium-Tritium (D-T) plasma, which is planned for 2020, the real-time protection of the first wall has been significantly improved. New optical relays have been installed on JET-ILW to take the images and the cameras outside of the biological shield. Additionally, new highly sensitive digital logarithmic NIR cameras were integrated into the protection scheme.

ITER relevant improvements of the protection imaging system are:

- Long distance optical relay (about 40m long) to take imaging cameras outside of the biological shield
- Mirror based optical design
- Optimised wavelength for T_{surf} measurements (NIR λ-range, λ=1.25μm): temperature independent spectral emissivity of W
- Less sensitivity of the measurements to the surface roughness
- Reduced max. relative error for the T_{surf} measurements
- Drawback: lower detection limit is $T_{surf} \approx 600^{\circ}C$
- Improved protection cameras
- InGaAs sensor – more sensitive in the range from 0.9μm to 1.7μm
- Logarithmic output- high dynamic range.

The system is calibrated with an in-vessel calibration light source. It is commissioned and is now ready for routine operation in the planned JET campaign and it will be particularly used

for further development of high-performance plasma scenarios. The real-time protection system is an essential tool for JET operation and the experience gained can contribute important ideas and methods to the design of the ITER plasma control system**.**

In addition to the technological aspect, the intensive preparation of the diverse software tools is in progress. The usefulness of generation of the dynamic background for real-time system during each pre-pulse stage in order to reduce the lower detection limit and correspondingly to increase the temperature range measured by NIR cameras, has been demonstrated.

A deeply revised version of the JUVIL software is now installed on JET. The JUVIL (JET Users Video Imaging Library) framework provides graphical components and functions for loading and post-processing of video data from various imaging systems.

For the identification of individual hot spots and for analysis of hots spot formation in relation to the diverse plasma parameter, a new software tool, Hotspot Editor, was developed and integrated into the JUVIL framework to enable easy tracking of the hot spots and of their evolution. The Hotspot Editor is now routinely used at JET for analysis of VTM events and alarms, edge plasma physics studies and post-pulse analysis of data required for the preparation of plasma pulses. It is to the credit of the Hotspot Editor that the number of the VTM alarms was significantly reduced during the last campaigns.

Notable progress has been achieved in the development of real time algorithms for hot spot detection as well as alarm handling strategy required for the wall protection. Reliable operation of the protection system based on video imaging was demonstrated in JET with ITER-like Wall. Safe landing of the plasma is achieved when hot spots are observed on the Be main chamber as well as in the divertor PFCs (bulk W and tungsten coated CFC tiles). It was demonstrated that the video imaging protection system can work properly under harsh conditions with neutrons and dust on the surface as well as layer deposits on the materials: about 2-3% of the plasma discharges were terminated by RTPS to avoid overheating of first wall materials within the last experimental campaigns.

Acknowledgements

This work has been carried out within the framework of the EUROfusion Consortium and has received funding from the Euratom research and training programme 2014-2018 and 2019-2020 under grant agreement No 633053. The views and opinions expressed herein do not necessarily reflect those of the European Commission.

References

[1] Matthews G.F. *et al* 2011 *Phys. Scr.* **T145** 014001
[2] Mertens, Ph. *et al* 2009 Phys. Scr. T138 014032
[3] Huber A. et al 2017 *Fusion Eng. Des.* Volume **123** 669-673, http://dx.doi.org/10.1016/j.fusengdes.2017.03.167
[4] NIT, New Imaging Technologies, http://new-imaging-technologies.com/en
[5] A.C. Maas et al., Fusion Engineering and Design **47** (1999) 247–265
[6] Alves D. et al 2012 Phys. Rev. ST Accel. Beams 15 054701.
[7] Huber A. *et al* 2018 Nucl. Fusion **58** 106021.
[8] Mayoral M.-L. et. al Nucl. Fusion **54** (2014) 033002 (14pp)
[9] Huber V. *et al* 2016 *Rev. Sci. Instrum.* **87** 11D430
[10] Biewer T.M. *et al* 2012 *Rev. Sci. Instrum.* **83** 10D505
[11] Marot L. et al 2007 *Rev. Sci. Instrum.* **78** 103507, http://dx.doi.org/10.1063/1.2800779
[12] Marot L. *et al* 2008 Surf. Sci. **602** 3375-3380,
[13] Marot L. *et al* 2009 J. Nucl. Mater. **390-391** 1135
[14] Litnovsky A. *et al* 2007 *Nucl. Fusion* **47** 833–838
[15] Mertens Ph. *et al* 2015 *Fusion Engineering and Design* **96–97** 129–135
[16] Mertens Ph *et al* 2019, Proc. 30th SOFT Conf., submitted to *Fusion Eng. and Des.*
[17] D.F.Valcárcel *et a*l 2014 Fusion Eng. Des. 89 243-258
[18] Huber V. *et al* 2017 Fusion Eng. Des. 123 979-985
[19] Silburn S. *et al* 2018 Calcam (Version 2.0.1), http://doi.org/10.5281/zenodo.2389481
[20] Nightingale M. P. S. *et al* 2009 AIP Conf. Proc. 1187, 213.
[21] Widdowson A. *et al* 2017 *Nucl. Mater. Energy* **12** 499–505
[22] Maier H. *et al* 2016 *Phys. Scr.* **T167** 014048